Top quark decay to a 125 GeV Higgs in the BLMSSM *

GAO Tie-Jun(高铁军)[1,2;1)] FENG Tai-Fu(冯太傅)[2] SUN Fei(孙飞)[3]
ZHANG Hai-Bin(张海斌)[3] ZHAO Shu-Min(赵树民)[2]

[1] State Key Laboratory of Theoretical Physics,
Institute of Theoretical Physics, Chinese Academy of Science, Beijing 100190, China
[2] Department of Physics, Hebei University, Baoding 071002, China
[3] Department of Physics, Dalian University of Technology, Dalian 116024, China

Abstract: In this paper, we calculate the rare top quark decay $t \to ch$ in a supersymmetric extension of the Standard Model where baryon and lepton numbers are local gauge symmetries. Adopting reasonable assumptions on the parameter space, we find that the branching ratios of $t \to ch$ can reach 10^{-3}, which could be detected in the near future.

Key words: supersymmetry, BLMSSM, top quark decays

PACS: 14.65.Ha, 12.60.Jv **DOI:** 10.1088/1674-1137/39/7/073101

1 Introduction

The top quark plays a special role in the Standard Model (SM) and holds great promise in revealing the secret of new physics beyond the SM. The currently-running Large Hadron Collider (LHC) is a top-quark factory, and provides a great opportunity to seek out rare top-quark decays. Among those rare processes, the flavor-changing neutral current (FCNC) decays $t \to ch$ deserve special attention, since the branching ratios (BRs) of these rare processes are strongly suppressed in the SM. In addition, ATLAS and CMS have reported significant excess events which are interpreted to be probably related to a neutral Higgs with mass $m_{h_0} \sim$124–126 GeV [1, 2]. This implies that the Higgs mechanism to break electroweak symmetry possibly has a solid experimental cornerstone.

In the framework of the SM, the possibility of detecting FCNC decays $t \to ch$ is essentially hopeless, since tree level FCNC involving quarks are forbidden by the gauge symmetries and particle content [3, 4]. In particular, it has recently been recognized that the BRs of the processes are much smaller [5, 6] than originally thought [7], being less than 10^{-13}. In extensions of the SM, the BRs for FCNC top decays can be orders of magnitude larger. For example, the authors of Ref.[8] study the $t \to ch$ process in the framework of the minimal supersymmetric extension of the Standard Model (MSSM), which includes the leading set of supersymmetric QCD and supersymmetric electroweak contributions, and get $Br^{\rm SUSY-EW}(t \to ch) \sim 10^{-8}$ and $Br^{\rm SUSY-QCD}(t \to ch) \sim 10^{-5}$. A new study of this process in the MSSM is discussed in Ref. [9]; with $\tan\beta$=1.5 or 35 and the mass of SUSY particles about the 1 or 2 TeV scale, the authors get a maximum branching ratio for $t \to ch$ of 3×10^{-6}, which is much smaller than previous results obtained before the advent of the LHC.

Physicists have been interested in the MSSM [10–13] for a long time. However, since there is an asymmetry between matter and antimatter in the universe, baryon number (B) should be broken. In addition, since heavy majorana neutrinos contained in the seesaw mechanism can induce tiny neutrino masses [14, 15] to explain the results obtained in a neutrino oscillation experiment, the lepton number (L) is also expected to be broken. A minimal supersymmetric extension of the SM with local gauged B and L (BLMSSM) is therefore more favoured [16, 17]. Since the new quarks predicted by this model are vector-like with respect to the strong, weak and electromagnetic interactions, to cancel anomalies, one obtains that their masses can be above 500 GeV without assuming large couplings to the Higgs doublets

Received 29 September 2014, Revised 20 January 2015

∗ Supported by National Natural Science Foundation of China (11275036), Open Project of State Key Laboratory of Mathematics-Mechanization (Y3KF311CJ1), Natural Science Foundation of Hebei Province of China (A2013201277), Natural Science Fund of Hebei University (2011JQ05, 2012-242)

1) E-mail: gao-t-j@foxmail.com

in this model. Therefore, there are no Landau poles for the Yukawa couplings here.

In the BLMSSM, B and L are spontaneously broken near the weak scale, proton decay is forbidden, and the three neutrinos get mass from the extended seesaw mechanism at tree level [3, 4, 16, 17]. Therefore, the desert between the grand unified scale and the electroweak scale is not necessary, which is the main motivation for the BLMSSM.

The CMS [18] and ATLAS [19] experiments at the LHC have searched for many possible MSSM signals and set very strong bounds on the gluino and squark masses with R-parity conservation. However, in the BLMSSM, the predictions and bounds for the collider experiments should be changed [16, 17, 20]. In addition, lepton number violation could be detected at the LHC from the decays of right-handed neutrinos [3, 4, 21], and we can also look for baryon number violation in the decays of squarks and gauginos [22]. Since there are some exotic fields, and there exist couplings between exotic quarks, exotic scalar quarks and SM quarks in the superpotential, this will cause flavor changing processes, so the BRs for FCNC top decays can be orders of magnitude larger than in the SM.

In this paper we analyze the corrections to the top-quark decay $t\to ch$ in the BLMSSM. This paper is constructed as follows. In Section 2, we present the main ingredients of the BLMSSM. In section 3, we present the theoretical calculation of the $t\to ch$ processes. Section 4 is devoted to the numerical analysis, and our conclusions are summarized in Section 5.

2 A supersymmtric extension of the SM where B and L are local gauge symmetries

The local gauge B and L is based on the gauge group $SU(3)_{\rm C}\otimes SU(2)_{\rm L}\otimes U(1)_{\rm Y}\otimes U(1)_{\rm B}\otimes U(1)_{\rm L}$. In the BLMSSM, to cancel the B and L anomalies, the exotic superfields should include the new quarks $\hat{Q}_4$, $\hat{U}_4^{\rm c}$, $\hat{D}_4^{\rm c}$, $\hat{Q}_5^{\rm c}$, $\hat{U}_5$, $\hat{D}_5$, and the new leptons $\hat{L}_4$, $\hat{E}_4^{\rm c}$, $\hat{N}_4^{\rm c}$, $\hat{L}_5^{\rm c}$, $\hat{E}_5$, $\hat{N}_5$. In addition, the new Higgs chiral superfields $\hat{\Phi}_{\rm B}$ and $\hat{\varphi}_{\rm B}$ acquire nonzero vacuum expectation values (VEVs) to break the baryon number spontaneously, and the superfields $\hat{\Phi}_{\rm L}$ and $\hat{\varphi}_{\rm L}$ acquire nonzero VEVs to break the lepton number spontaneously. The model also introduces the superfields $\hat{X}$, $\hat{X}'$ to avoid stability for the exotic quarks. Actually, the lightest superfields could be a candidate for dark matter. The properties of these superfields in the BLMSSM are summarized in Table 1, where B_4 and L_4 stand for the baryon and lepton number of exotic quark and lepton superfields. In our case we will take $B_4=L_4=\dfrac{3}{2}$ [23].

Table 1. Properties of superfields in the BLMSSM.

superfield	$SU(3)$	$SU(2)$	$U(1)_{\rm Y}$	$U(1)_{\rm B}$	$U(1)_{\rm L}$
$\hat{Q}_4$	3	2	1/6	B_4	0
$\hat{U}_4^{\rm c}$	$\bar{3}$	1	−2/3	$-B_4$	0
$\hat{D}_4^{\rm c}$	$\bar{3}$	1	1/3	$-B_4$	0
$\hat{Q}_5^{\rm c}$	$\bar{3}$	2	−1/6	$-(1+B_4)$	0
$\hat{U}_5$	3	1	2/3	$1+B_4$	0
$\hat{D}_5$	3	1	−1/3	$1+B_4$	0
$\hat{L}_4$	1	2	−1/2	0	L_4
$\hat{E}_4^{\rm c}$	1	1	1	0	$-L_4$
$\hat{N}_4^{\rm c}$	1	1	0	0	$-L_4$
$\hat{L}_5^{\rm c}$	1	2	1/2	0	$-(3+L_4)$
$\hat{E}_5$	1	1	−1	0	$3+L_4$
$\hat{N}_5$	1	1	0	0	$3+L_4$
$\hat{\Phi}_{\rm B}$	1	1	0	1	0
$\hat{\varphi}_{\rm B}$	1	1	0	−1	0
$\hat{\Phi}_{\rm L}$	1	1	0	0	−2
$\hat{\varphi}_{\rm L}$	1	1	0	0	2
$\hat{X}$	1	1	0	$2/3+B_4$	0
$\hat{X}'$	1	1	0	$-(2/3+B_4)$	0

In the BLMSSM, the superpotential is written as [23, 24]

$$\mathcal{W}_{\rm BLMSSM}=\mathcal{W}_{\rm MSSM}+\mathcal{W}_{\rm B}+\mathcal{W}_{\rm L}+\mathcal{W}_{\rm X}, \tag{1}$$

where $\mathcal{W}_{\rm MSSM}$ is the MSSM superpotential, and the concrete forms of $\mathcal{W}_{\rm B}$, $\mathcal{W}_{\rm L}$ and $\mathcal{W}_{\rm X}$ are

$$\begin{aligned}
\mathcal{W}_{\rm B} =\ & \lambda_Q\hat{Q}_4\hat{Q}_5^{\rm c}\hat{\Phi}_{\rm B}+\lambda_{\rm U}\hat{U}_4^{\rm c}\hat{U}_5\hat{\varphi}_{\rm B}+\lambda_{\rm D}\hat{D}_4^{\rm c}\hat{D}_5\hat{\varphi}_{\rm B}\\
&+\mu_{\rm B}\hat{\Phi}_{\rm B}\hat{\varphi}_{\rm B}+Y_{\rm u_4}\hat{Q}_4\hat{H}_{\rm u}\hat{U}_4^{\rm c}+Y_{\rm d_4}\hat{Q}_4\hat{H}_{\rm d}\hat{D}_4^{\rm c}\\
&+Y_{\rm u_5}\hat{Q}_5^{\rm c}\hat{H}_{\rm d}\hat{U}_5+Y_{\rm d_5}\hat{Q}_5^{\rm c}\hat{H}_{\rm u}\hat{D}_5,\\
\mathcal{W}_{\rm L} =\ & Y_{\rm e_4}\hat{L}_4\hat{H}_{\rm d}\hat{E}_4^{\rm c}+Y_{\nu_4}\hat{L}_4\hat{H}_{\rm u}\hat{\nu}_4^{\rm c}+Y_{\rm e_5}\hat{L}_5^{\rm c}\hat{H}_{\rm u}\hat{E}_5\\
&+Y_{\nu_5}\hat{L}_5^{\rm c}\hat{H}_{\rm d}\hat{\nu}_5+Y_{\nu}\hat{L}\hat{H}_{\rm u}\hat{\nu}^{\rm c}+\lambda_{\nu^{\rm c}}\hat{\nu}^{\rm c}\hat{\nu}^{\rm c}\hat{\varphi}_{\rm L}+\mu_{\rm L}\hat{\Phi}_{\rm L}\hat{\varphi}_{\rm L},\\
\mathcal{W}_{\rm X} =\ & \lambda_1\hat{Q}\hat{Q}_5^{\rm c}\hat{X}+\lambda_2\hat{U}^{\rm c}\hat{U}_5\hat{X}'+\lambda_3\hat{D}^{\rm c}\hat{D}_5\hat{X}'+\mu_{\rm X}\hat{X}\hat{X}'.
\end{aligned} \tag{2}$$

We can see that since $\mathcal{W}_{\rm X}$ contains superfields X and Q_5 (U_5, D_5 and X') which couple to all generations of SM quarks, FCNC processes can be generated.

Correspondingly, the soft breaking terms $\mathcal{L}_{\rm soft}$ are generally given as

$$\begin{aligned}
\mathcal{L}_{\rm soft} =\ & \mathcal{L}_{\rm soft}^{\rm MSSM}-(m^2_{\tilde{\nu}^{\rm c}})_{\rm IJ}\tilde{\nu}_{\rm I}^{\rm c*}\tilde{\nu}_{\rm J}^{\rm c}-m^2_{\tilde{\rm Q}_4}\tilde{Q}_4^{\dagger}\tilde{Q}_4\\
&-m^2_{\tilde{\rm U}_4}\tilde{U}_4^{\rm c*}\tilde{U}_4^{\rm c}-m^2_{\tilde{\rm D}_4}\tilde{D}_4^{\rm c*}\tilde{D}_4^{\rm c}-m^2_{\tilde{\rm Q}_5}\tilde{Q}_5^{\rm c\dagger}\tilde{Q}_5^{\rm c}\\
&-m^2_{\tilde{\rm U}_5}\tilde{U}_5^{*}\tilde{U}_5-m^2_{\tilde{\rm D}_5}\tilde{D}_5^{*}\tilde{D}_5-m^2_{\tilde{\rm L}_4}\tilde{L}_4^{\dagger}\tilde{L}_4-m^2_{\tilde{\nu}_4}\tilde{\nu}_4^{\rm c*}\tilde{\nu}_4^{\rm c}\\
&-m^2_{\tilde{\rm E}_4}\tilde{e}_4^{\rm c*}\tilde{e}_4^{\rm c}-m^2_{\tilde{\rm L}_5}\tilde{L}_5^{\rm c\dagger}\tilde{L}_5^{\rm c}-m^2_{\tilde{\nu}_5}\tilde{\nu}_5^{*}\tilde{\nu}_5-m^2_{\tilde{\rm E}_5}\tilde{e}_5^{*}\tilde{e}_5\\
&-m^2_{\Phi_{\rm B}}\Phi_{\rm B}^{*}\Phi_{\rm B}-m^2_{\varphi_{\rm B}}\varphi_{\rm B}^{*}\varphi_{\rm B}-m^2_{\Phi_{\rm L}}\Phi_{\rm L}^{*}\Phi_{\rm L}\\
&-m^2_{\varphi_{\rm L}}\varphi_{\rm L}^{*}\varphi_{\rm L}-\Big(m_{\rm B}\lambda_{\rm B}\lambda_{\rm B}+m_{\rm L}\lambda_{\rm L}\lambda_{\rm L}+{\rm h.c.}\Big)\\
&+\Big\{A_{\rm u_4}Y_{\rm u_4}\tilde{Q}_4H_{\rm u}\tilde{U}_4^{\rm c}+A_{\rm d_4}Y_{\rm d_4}\tilde{Q}_4H_{\rm d}\tilde{D}_4^{\rm c}\\
&+A_{\rm u_5}Y_{\rm u_5}\tilde{Q}_5^{\rm c}H_{\rm d}\tilde{U}_5+A_{\rm d_5}Y_{\rm d_5}\tilde{Q}_5^{\rm c}H_{\rm u}\tilde{D}_5
\end{aligned}$$

$$
\begin{aligned}
&+A_{\rm BQ}\lambda_{\rm Q}\tilde{Q}_4\tilde{Q}^{\rm c}_5\Phi_{\rm B}+A_{\rm BU}\lambda_{\rm U}\tilde{U}^{\rm c}_4\tilde{U}_5\varphi_{\rm B}\\
&+A_{\rm BD}\lambda_{\rm D}\tilde{D}^{\rm c}_4\tilde{D}_5\varphi_{\rm B}+B_{\rm B}\mu_{\rm B}\Phi_{\rm B}\varphi_{\rm B}+{\rm h.c.}\Big\}\\
&+\Big\{A_{{\rm e}_4}Y_{{\rm e}_4}\tilde{L}_4H_{\rm d}\tilde{E}^{\rm c}_4+A_{\nu_4}Y_{\nu_4}\tilde{L}_4H_{\rm u}\tilde{\nu}^{\rm c}_4\\
&+A_{{\rm e}_5}Y_{{\rm e}_5}\tilde{L}^{\rm c}_5H_{\rm u}\tilde{E}_5+A_{\nu_5}Y_{\nu_5}\tilde{L}^{\rm c}_5H_{\rm d}\tilde{\nu}_5\\
&+A_{\nu}Y_{\nu}\tilde{L}H_{\rm u}\tilde{\nu}^{\rm c}+A_{\nu^{\rm c}}\lambda_{\nu^{\rm c}}\tilde{\nu}^{\rm c}\tilde{\nu}^{\rm c}\varphi_{\rm L}+B_{\rm L}\mu_{\rm L}\Phi_{\rm L}\varphi_{\rm L}\\
&+{\rm h.c.}\Big\}+\Big\{A_1\lambda_1\tilde{Q}\tilde{Q}^{\rm c}_5X+A_2\lambda_2\tilde{U}^{\rm c}\tilde{U}_5X'\\
&+A_3\lambda_3\tilde{D}^{\rm c}\tilde{D}_5X'+B_{\rm X}\mu_{\rm X}XX'+{\rm h.c.}\Big\},
\end{aligned}\tag{3}
$$

with $\mathcal{L}^{\rm MSSM}_{\rm soft}$ representing the soft breaking terms of the MSSM, and $\lambda_{\rm B}$, $\lambda_{\rm L}$ being gauginos of $U(1)_{\rm B}$ and $U(1)_{\rm L}$, respectively.

To break the local gauge symmetry $SU(2)_{\rm L}\otimes U(1)_{\rm Y}\otimes U(1)_{\rm B}\otimes U(1)_{\rm L}$ down to the electromagnetic symmetry $U(1)_{\rm e}$, the $SU(2)_{\rm L}$ doublets $H_{\rm u}$, $H_{\rm d}$ and the $SU(2)_{\rm L}$ singlets $\Phi_{\rm B}$, $\varphi_{\rm B}$, $\Phi_{\rm L}$, $\varphi_{\rm L}$ should have nonzero VEVs $\upsilon_{\rm u}$, $\upsilon_{\rm d}$, $\upsilon_{\rm B}$, $\overline{\upsilon}_{\rm B}$, and $\upsilon_{\rm L}$, $\overline{\upsilon}_{\rm L}$ respectively.

$$
\begin{aligned}
H_{\rm u} &= \begin{pmatrix} H^+_{\rm u} \\ \frac{1}{\sqrt{2}}\Big(\upsilon_{\rm u}+H^0_{\rm u}+{\rm i}P^0_{\rm u}\Big)\end{pmatrix},\\
H_{\rm d} &= \begin{pmatrix} \frac{1}{\sqrt{2}}\Big(\upsilon_{\rm d}+H^0_{\rm d}+{\rm i}P^0_{\rm d}\Big) \\ H^-_{\rm d}\end{pmatrix},\\
\Phi_{\rm B} &= \frac{1}{\sqrt{2}}\Big(\upsilon_{\rm B}+\Phi^0_{\rm B}+{\rm i}P^0_{\rm B}\Big),\\
\varphi_{\rm B} &= \frac{1}{\sqrt{2}}\Big(\overline{\upsilon}_{\rm B}+\varphi^0_{\rm B}+{\rm i}\overline{P}^0_{\rm B}\Big),\\
\Phi_{\rm L} &= \frac{1}{\sqrt{2}}\Big(\upsilon_{\rm L}+\Phi^0_{\rm L}+{\rm i}P^0_{\rm L}\Big),\\
\varphi_{\rm L} &= \frac{1}{\sqrt{2}}\Big(\overline{\upsilon}_{\rm L}+\varphi^0_{\rm L}+{\rm i}\overline{P}^0_{\rm L}\Big).
\end{aligned}\tag{4}
$$

The mass matrices of the Higgs, exotic quarks and exotic scalar quarks were obtained in our previous work [23]; here, we list some useful results.

In four-component Dirac spinors, the mass matrix for exotic charge-2/3 quarks is

$$
\begin{aligned}
-L^{\rm mass}_{\rm t''} &= \Big(\bar{t}''_{\rm 4R},\,\bar{t}''_{\rm 5R}\Big)\begin{pmatrix} \frac{1}{\sqrt{2}}Y_{\rm u_4}\upsilon_{\rm u}, & -\frac{1}{\sqrt{2}}\lambda_{\rm Q}\upsilon_{\rm B} \\ -\frac{1}{\sqrt{2}}\lambda_{\rm u}\bar{\upsilon}_{\rm B}, & \frac{1}{\sqrt{2}}Y_{\rm u_5}\upsilon_{\rm d}\end{pmatrix}\\
&\quad\times\begin{pmatrix} t''_{\rm 4L} \\ t''_{\rm 5L}\end{pmatrix}+{\rm h.c.}
\end{aligned}\tag{5}
$$

which can be diagonalized by the unitary transformations

$$
\begin{pmatrix} t'_{\rm 4L} \\ t'_{\rm 5L}\end{pmatrix}=U^{\dagger}_{\rm t'}\cdot\begin{pmatrix} t''_{\rm 4L} \\ t''_{\rm 5L}\end{pmatrix},\begin{pmatrix} t'_{\rm 4R} \\ t'_{\rm 5R}\end{pmatrix}=W^{\dagger}_{\rm t'}\cdot\begin{pmatrix} t''_{\rm 4R} \\ t''_{\rm 5R}\end{pmatrix},\tag{6}
$$

giving

$$
W^{\dagger}_{\rm t'}\cdot\begin{pmatrix} \frac{1}{\sqrt{2}}Y_{\rm u_4}\upsilon_{\rm u}, & -\frac{1}{\sqrt{2}}\lambda_{\rm Q}\upsilon_{\rm B} \\ -\frac{1}{\sqrt{2}}\lambda_{\rm u}\bar{\upsilon}_{\rm B}, & \frac{1}{\sqrt{2}}Y_{\rm u_5}\upsilon_{\rm d}\end{pmatrix}\cdot U_{\rm t'}={\rm diag}(m_{\rm t_4},m_{\rm t_5}).\tag{7}
$$

Similarly, the concrete expressions for 4×4 mass squared matrices $M^2_{\tilde{\rm t}'}$ of exotic charge-2/3 scalar quarks $\tilde{t}''^{\rm T}=(\tilde{Q}^1_4,\,\tilde{U}^{\rm c*}_4,\,\tilde{Q}^{\rm 2c*}_5,\tilde{U}_5)$ are given in appendix B of Ref. [23]; these can be diagonalized by the unitary transformation

$$
\tilde{t}''_{\rm i}=Z^{\rm ij}_{\tilde{\rm t}'}\tilde{t}'_{\rm j}.\tag{8}
$$

Using the scalar potential and the soft breaking terms, the mass squared matrix for X,X' can be written as

$$
-L^{\rm mass}_{\rm X}=\begin{pmatrix} X^* & X'\end{pmatrix}\begin{pmatrix} \mu^2_{\rm X}+S_{\rm X} & -B_{\rm X}\mu_{\rm X} \\ -B_{\rm X}\mu_{\rm X} & \mu^2_{\rm X}-S_{\rm X}\end{pmatrix}\begin{pmatrix} X \\ X'\end{pmatrix},\tag{9}
$$

where $S_{\rm X}=\frac{g^2_{\rm B}}{2}\left(\frac{2}{3}+B_4\right)(\upsilon^2_{\rm B}-\overline{\upsilon}^2_{\rm B})$. It can be diagonalized by the unitary transformation $Z_{\rm X}$

$$
Z^{\dagger}_{\rm X}\begin{pmatrix} \mu^2_{\rm X}+S_{\rm X} & -B_{\rm X}\mu_{\rm X} \\ -B_{\rm X}\mu_{\rm X} & \mu^2_{\rm X}-S_{\rm X}\end{pmatrix}Z_{\rm X}={\rm diag}(m^2_{\rm X_1},m^2_{\rm X_2}).\tag{10}
$$

In addition, the four-component Dirac spinor $\widetilde{X}$ is defined as $\widetilde{X}=(\psi_{\rm X},\bar{\psi}_{\rm X'})^{\rm T}$, with the mass term $\mu_{\rm X}\widetilde{X}\overline{\widetilde{X}}$.

The flavor conservative couplings between the lightest neutral Higgs and charge-2/3 exotic quarks are

$$
\begin{aligned}
\mathcal{L}_{\rm Ht't'} &= \frac{1}{\sqrt{2}}\sum^{2}_{i,j=1}\Big\{\Big[Y_{\rm u_4}(W^{\dagger}_{\rm t})_{i2}(U_{\rm t})_{1j}\cos\alpha\\
&\quad+Y_{\rm u_5}(W^{\dagger}_{\rm t})_{i1}(U_{\rm t})_{2j}\sin\alpha\Big]h^0\overline{t'}_iP_{\rm L}t'_j\\
&\quad+\Big[Y_{\rm u_4}(U^{\dagger}_{\rm t})_{i1}(W_{\rm t})_{2j}\cos\alpha\\
&\quad+Y_{\rm u_5}(U^{\dagger}_{\rm t})_{i2}(W_{\rm t})_{1j}\sin\alpha\Big]h^0\overline{t'}_iP_{\rm R}t'_j,
\end{aligned}\tag{11}
$$

with α defined as

$$
\begin{pmatrix} H^0 \\ h^0\end{pmatrix}=\begin{pmatrix} \cos\alpha & \sin\alpha \\ -\sin\alpha & \cos\alpha\end{pmatrix}\begin{pmatrix} H^0_{\rm d} \\ H^0_{\rm u}\end{pmatrix}.\tag{12}
$$

The couplings between the lightest neutral Higgs and exotic scalar quarks are

$$
\mathcal{L}_{\rm H\tilde{t}'^*_i\tilde{t}'}=\sum^{4}_{i,j}\Big[\xi^{\rm S}_{{\rm u}ij}\cos\alpha-\xi^{\rm S}_{{\rm d}ij}\sin\alpha\Big]h^0\tilde{t}'^*_i\tilde{t}'_j,\tag{13}
$$

with $\xi^{\rm S}_{{\rm u}ij}$ and $\xi^{\rm S}_{{\rm d}ij}$ as defined in Appendix C of Ref. [23].

In the mass basis, we obtain the couplings of quark-exotic quark and the X as

$$-\lambda_1(W_{t'})_{i2}(Z_X)_{1j}X_j\bar{t}'_iP_Lu-\lambda_2(U^\dagger_{t'})_{2i}(Z_X)_{2j}X_j\bar{u}P_Lt'_i+\text{h.c.} \tag{14}$$

and the couplings between up type quarks and the superpartners $\widetilde{t}'$, $\widetilde{X}$ are

$$-\lambda_1(Z^\dagger_{\tilde{t}'})_{i3}\tilde{t}'_i\bar{u}P_L\tilde{X}-\lambda_2(Z^\dagger_{\tilde{t}'})_{i4}\tilde{t}'_i\bar{\tilde{X}}P_Lu+\text{h.c.} \tag{15}$$

3 Theoretical calculation of the t → ch process

In this section, we present one-loop radiative corrections to the rare decay t→ch in the BLMSSM. For this process, it is convenient to define an effective interaction vertex [8]:

$$-iT=-ig\bar{c}(p)(F_LP_L+F_RP_R)t(p'), \tag{16}$$

where p' is the momentum of the initial top quark, p is the momentum of the final state charm quark, and the form factors F_L, F_R follow from an explicit calculation of vertices and mixed self-energies, with

$$\begin{aligned} F_L&=F_L^{\rm BLMSSM}+F_L^{\rm MSSM}+F_L^{\rm SM},\\ F_R&=F_R^{\rm BLMSSM}+F_R^{\rm MSSM}+F_R^{\rm SM}. \end{aligned} \tag{17}$$

Here the analytical expressions of the MSSM $F_{L,R}^{\rm MSSM}$ can be found in Ref. [8]. Since the SM contribution is very small, about 10^{-13} [7], we ignore the SM form factors. In the following, we will discuss the contributions of the BLMSSM $F_{L,R}^{\rm BLMSSM}$ in detail.

The relevant one-loop vertex diagrams of the BLMSSM are drawn in Fig. 1.

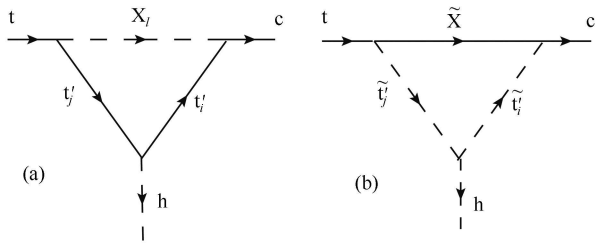

Fig. 1. Vertex diagrams contributing to the t→ch decay in the BLMSSM.

We can see that the FCNC transitions of new physics are mediated by the exotic up type quark t′, the neutral scalar particle X_i and their superpartners $\widetilde{t}'$, $\widetilde{X}$. The contribution to the form factors can be obtained by direct calculation.

In the equations below, $m_{t'}$, m_X, $m_{\tilde{t}'}$, $m_{\tilde{X}}$ denote the mass of the exotic quarks t′, the mass of the scalar particle X_i, and the mass of their superpartners $\widetilde{t}'$, $\widetilde{X}$ respectively. B_i, C_{ij} are the coefficients of the Lorentz-covariant tensors in the standard scalar Passarino-Veltman integrals (Eq. (4.7) in Ref. [25]), and can be calculated using 'LoopTools'.

In Fig. 1(a), when one-loop diagrams are composed by the neutral scalar particles X_i and charge-2/3 new quarks t′, the contributions to the form factors F_L^a and F_R^a are formulated as

$$\begin{aligned} F_L^a &= \frac{i}{16\pi^2}\sum_{i,j,\ l}(-a_1m_c(b_1h_2m_tC_2\\ &\quad+b_2h_1m_{t'_i}(C_0+C_1+2C_2)+3b_2h_2m_{t'_j}C_2))\\ &\quad+a_2b_2(h_1B_0+(h_1m^2_{t'_i}+h_2m_{t'_i}m_{t'_j})C_0)\\ &\quad+a_2b_1m_t(h_2m_{t'_i}(C_0+C_1+C_2)+h_1m_{t'_j}(C_1+C_2))\\ &\quad+a_2b_2h_1{m_c}^2C_2,\\ F_R^a &= \frac{i}{16\pi^2}\sum_{i,j,\ l}(-a_2m_c(b_1h_2m_{t'_i}(C_0+C_1+2C_2)\\ &\quad+b_1h_1m_{t'_j}(C_1+2C_2)+b_2h_1m_tC_2))\\ &\quad+a_1b_1(h_2B_0+(h_1m_{t'_i}m_{t'_j}+h_2m^2_{t'_i})C_0)\\ &\quad+a_1b_2m_t(h_1m_{t'_i}(C_0+C_1+C_2)+h_2m_{t'_j}(C_1+C_2))\\ &\quad+a_1b_1h_2{m_c}^2C_2, \end{aligned} \tag{18}$$

with the Passarino-Veltman integrals

$$\begin{aligned} B_0 &= B_0(p^2,m^2_{t'_j},m^2_{X_l}),\\ C_0 &= C_0\Big(p^2,(2p-p')^2,(p-p')^2,m^2_{t'_j},m^2_{X_l},m^2_{t'_i}\Big),\\ C_{1,2} &= C_{1,2}\Big((p-p')^2,(2p-p')^2,p^2,m^2_{t'_i},m^2_{t'_j},m^2_{X_l}\Big), \end{aligned} \tag{19}$$

and the relevant coefficients

$$\begin{aligned} a_1 &= \lambda_1^*(W^\dagger_{t'})_{2i}(Z^\dagger_X)_{l1},\quad a_2=\lambda_2(U^\dagger_{t'})_{2i}(Z_X)_{2l},\\ b_1 &= \lambda_2^*(U_{t'})_{j2}(Z^\dagger_X)_{l2},\quad b_2=\lambda_1(W_{t'})_{j2}(Z_X)_{1l},\\ h_1 &= Y_{u_4}(U^\dagger_{t'})_{i1}(W_{t'})_{2j}\cos\alpha+Y_{u_5}(U^\dagger_{t'})_{i2}(W_{t'})_{1j}\sin\alpha,\\ h_2 &= Y_{u_4}(W^\dagger_{t'})_{i2}(U_{t'})_{1j}\cos\alpha+Y_{u_5}(W^\dagger_{t'})_{i1}(U_{t'})_{2j}\sin\alpha. \end{aligned} \tag{20}$$

In Fig. 1(b), when the one-loop diagrams are composed by the superpartners $\widetilde{t}'$ and $\widetilde{X}$, F_L^b and F_R^b are formulated as

$$\begin{aligned} F_L^b &= \frac{i}{16\pi^2}\sum_{i,j}(a_4b_4m_{\tilde{X}}C_0-a_3b_4m_cC_1-a_4b_3m_tC_2)\\ &\quad\times(\cos\alpha\xi_u-\sin\alpha\xi_d),\\ F_R^b &= \frac{i}{16\pi^2}\sum_{i,j}(a_4b_4m_{\tilde{X}}C_0-a_3b_4m_cC_1-a_4b_3m_tC_2)\\ &\quad\times(\cos\alpha\xi_u-\sin\alpha\xi_d), \end{aligned} \tag{21}$$

with

$$\begin{aligned} C_0 &= C_0\Big(p^2,p'^2,(p-p')^2,m^2_{\tilde{t}'_i},m^2_{\tilde{X}},m^2_{\tilde{t}'_j}\Big),\\ C_{1,2} &= C_{1,2}\Big(p^2,(p-p')^2,p'^2,m^2_{\tilde{X}},m^2_{\tilde{t}'_i},m^2_{\tilde{t}'_j}\Big), \end{aligned} \tag{22}$$

and the relevant coefficients are

$$\begin{aligned} a_3 &= \lambda_2^*(Z_{\tilde{t}'}^\dagger)_{i4}, \quad a_4=\lambda_1(Z_{\tilde{t}'}^\dagger)_{i3}, \\ b_3 &= \lambda_1^*(Z_{\tilde{t}'})_{3j}, \quad b_4=\lambda_2(Z_{\tilde{t}'})_{4j}. \end{aligned} \tag{23}$$

In Fig. 2 we present the relevant self-energy diagrams of the rare decay t→ch in the BLMSSM.

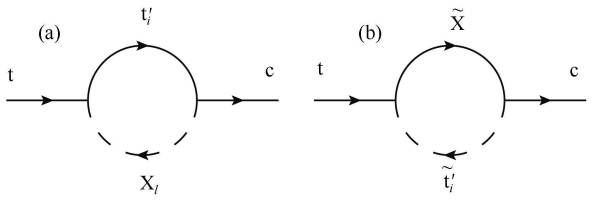

Fig. 2. Self-energy diagrams contributing to the t→ch decay in the BLMSSM.

As in Ref. [8], it is convenient to define the following structure:

$$\begin{aligned} \Sigma_{\rm tc}(k) \equiv\ & \not{k}\Sigma_{\rm L}(k^2)P_{\rm L}+\not{k}\Sigma_{\rm R}(k^2)P_{\rm R}+m_{\rm t}(\Sigma_{\rm Ls}(k^2)P_{\rm L} \\ & +\Sigma_{\rm Rs}(k^2)P_{\rm R}). \end{aligned} \tag{24}$$

Here, the factor $m_{\rm t}$ is inserted only to preserve the same dimensionality for the different Σ [8]. The effective interaction vertex of the mixed self-energy diagrams can be taken as the following general form in terms of the various Σ.

$$\begin{aligned} -{\rm i}T_{\rm Sc} =\ & \frac{-{\rm i}gm_{\rm t}}{2m_{\rm W}\sin\beta}\frac{1}{m_{\rm c}^2-m_{\rm t}^2}\bar{c}(p)\Big\{P_{\rm L}\cos\alpha[m_{\rm c}^2\Sigma_{\rm R}(m_{\rm c}^2) \\ & +m_{\rm c}m_{\rm t}(\Sigma_{\rm Rs}(m_{\rm c}^2)+\Sigma_{\rm L}(m_{\rm c}^2))+m_{\rm t}^2\Sigma_{\rm Ls}(m_{\rm c}^2)] \\ & +P_{\rm R}\cos\alpha[L\leftrightarrow R]\Big\}t(p'), \\ -{\rm i}T_{\rm St} =\ & \frac{-{\rm i}gm_{\rm c}}{2m_{W}\sin\beta}\frac{m_{\rm t}}{m_{\rm c}^2-m_{\rm t}^2}\bar{c}(p)\Big\{P_{\rm L}\cos\alpha[m_{\rm t}(\Sigma_{\rm L}(m_{\rm t}^2) \\ & +\Sigma_{\rm Rs}(m_{\rm t}^2))+m_{\rm c}(\Sigma_{\rm R}(m_{\rm t}^2)+\Sigma_{\rm Ls}(m_{\rm t}^2))] \\ & +P_{\rm R}\cos\alpha[L\leftrightarrow R]\Big\}t(p'). \end{aligned} \tag{25}$$

Comparing with Eq. (16), the corresponding contribution to the form factors $F_{\rm L}$ and $F_{\rm R}$ is transparent.

Using the couplings above, we can get the Σ of the self-energy diagrams in Fig. 2(a) as

$$\begin{aligned} \Sigma_{\rm L}(k^2) =\ & \frac{\rm i}{16\pi^2}\sum_{i,\ l}a_1b_2(B_0(k^2,m_{{\rm X}_l}^2,m_{\rm t'}^2) \\ & +B_1(k^2,m_{{\rm X}_l}^2,m_{\rm t'}^2)), \\ \Sigma_{\rm R}(k^2) =\ & \frac{\rm i}{16\pi^2}\sum_{i,\ l}a_2b_1(B_0(k^2,m_{{\rm X}_l}^2,m_{\rm t'}^2) \\ & +B_1(k^2,m_{{\rm X}_l}^2,m_{\rm t'}^2)), \\ m_{\rm t}\Sigma_{\rm Ls}(k^2) =\ & \frac{\rm i}{16\pi^2}\sum_{i,\ l}a_2b_2m_{\rm t'}B_0(k^2,m_{{\rm X}_l}^2,m_{\rm t'}^2), \\ m_{\rm t}\Sigma_{\rm Rs}(k^2) =\ & \frac{\rm i}{16\pi^2}\sum_{i,\ l}a_1b_1m_{\rm t'}B_0(k^2,m_{{\rm X}_l}^2,m_{\rm t'}^2). \end{aligned} \tag{26}$$

where $B_{0,1}$ are the two-point functions. Similarly, the Σ of the self-energy diagrams in Fig. 2(b) have the form:

$$\begin{aligned} \Sigma_{\rm L}(k^2) =\ & \frac{\rm i}{16\pi^2}\sum_{i}a_3b_4(B_0(k^2,m_{\tilde{\rm t}'}^2,m_{\tilde{\rm X}}^2) \\ & +B_1(k^2,m_{\tilde{\rm t}'}^2,m_{\tilde{\rm X}}^2)), \\ \Sigma_{\rm R}(k^2) =\ & \frac{\rm i}{16\pi^2}\sum_{i}a_4b_3(B_0(k^2,m_{\tilde{\rm t}'}^2,m_{\tilde{\rm X}}^2) \\ & +B_1(k^2,m_{\tilde{\rm t}'}^2,m_{\tilde{\rm X}}^2)), \\ m_{\rm t}\Sigma_{\rm Ls}(k^2) =\ & \frac{\rm i}{16\pi^2}\sum_{i}a_4b_4m_{\tilde{\rm t}'}B_0(k^2,m_{\tilde{\rm t}'}^2,m_{\tilde{\rm X}}^2), \\ m_{\rm t}\Sigma_{\rm Rs}(k^2) =\ & \frac{\rm i}{16\pi^2}\sum_{i}a_3b_3m_{\tilde{\rm t}'}B_0(k^2,m_{\tilde{\rm t}'}^2,m_{\tilde{\rm X}}^2). \end{aligned} \tag{27}$$

4 Numerical analysis

In the general case, the partial widths of the t→ch process are [8]

$$\begin{aligned} \Gamma({\rm t}\to{\rm ch}) =\ & \frac{g^2}{32\pi m_{\rm t}^3}\lambda^{1/2}(m_{\rm t}^2,m_{\rm h}^2,m_{\rm c}^2)\Big[(m_{\rm t}^2+m_{\rm c}^2-m_{\rm h}^2) \\ & \times\left(|F_{\rm L}|^2+|F_{\rm R}|^2\right)+2m_{\rm t}m_{\rm c}(F_{\rm L}F_{\rm R}^*+F_{\rm L}^*F_{\rm R})\Big], \end{aligned} \tag{28}$$

where $\lambda(x^2,\ y^2,\ z^2)=(x^2-(y+z)^2)(x^2-(y-z)^2)$ is the usual Källen function, and as mentioned in Eq. (17), $F_{\rm L,R}=F_{\rm L,R}^{\rm BLMSSM}+F_{\rm L,R}^{\rm MSSM}+F_{\rm L,R}^{\rm SM}$.

To compute the branching ratio, we take the SM charged-current two-body decay t→bW to be the dominant t-quark decay mode, which has $\Gamma({\rm t}\to{\rm bW}^+)=1.466|V_{\rm tb}|^2$. The branching ratio can be approximated by

$$Br({\rm t}\to{\rm ch})=\frac{\Gamma({\rm t}\to{\rm ch})}{\Gamma({\rm t}\to{\rm bW}^+)}. \tag{29}$$

To reduce the number of free parameters in our numerical analysis, the parameters are adopted as in Ref. [23, 24]. With this choice, it is easy for the 2×2 CP-even Higgs mass squared matrix to predict the lightest eigenvector with a mass of 125.9 GeV, and the choice also fits the behavior of h→γγ and h→VV* (V=Z, W) well [23]:

$$\begin{aligned} B_4 &= \frac{3}{2},\ \ v_{\rm B_t}=\sqrt{v_{\rm B}^2+\bar{v}_{\rm B}^2}=3\ {\rm TeV}, \\ \tan\beta &= \tan\beta_{\rm B}=2, \\ m_{\tilde{\rm U}_4} &= m_{\tilde{\rm Q}_5}=m_{\tilde{\rm U}_5}=1\ {\rm TeV}, \\ A_{\rm u_4} &= A_{\rm u_5}=500\ {\rm GeV}, \\ A_{\rm BU} &= 1\ {\rm TeV},\ \ \lambda_{\rm u}=0.5, \\ Y_{\rm u_4} &= 0.76Y_{\rm t},\ \ Y_{\rm d_4}=0.7Y_{\rm b}, \end{aligned}$$

$$\begin{aligned} Y_{u_5} &= 0.7Y_b,\ \ Y_{d_5}=0.13Y_t, \\ \mu &= -800\ \text{GeV} \\ B_X &= 500\ \text{GeV},\ \ \mu_X=2\ \text{TeV}, \end{aligned} \tag{30}$$

choosing $m_{Z_B} = 1$ TeV, $\mu_B = 500$ GeV, $\lambda_Q = 0.5$, and $A_{BQ} = 1$ TeV. We plot in Fig. 3 the BRs of $t \to ch$ versus $m_{\tilde{Q}_4}$, with the solid line, dashed line and dotted line corresponding to $\lambda_1 = \lambda_2$=0.6, 0.4 and 0.2 respectively. We can see that the BRs decrease as $m_{\tilde{Q}_4}$ runs from 700 GeV to 1300 GeV, and increase when $\lambda_1 = \lambda_2$ increases, because $m_{\tilde{Q}_4}$ is the mass parameter of the exotic scalar quarks, and λ_1, λ_2 are proportional to the coupling coefficient. In addition, when $m_{\tilde{Q}_4} \geqslant 1100$ GeV, the BRs tend to the results of the MSSM.

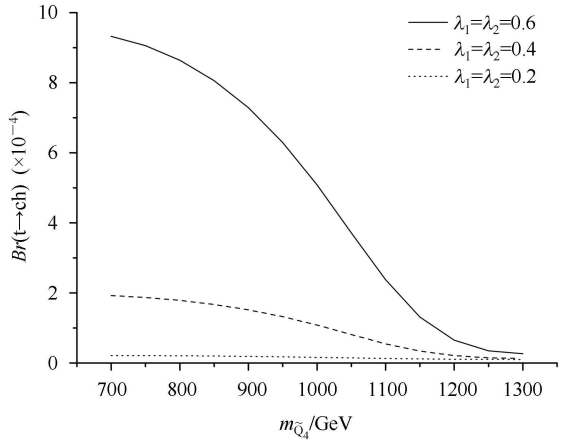

Fig. 3. Variation of t→ch branching ratio with $m_{\tilde{Q}_4}$.

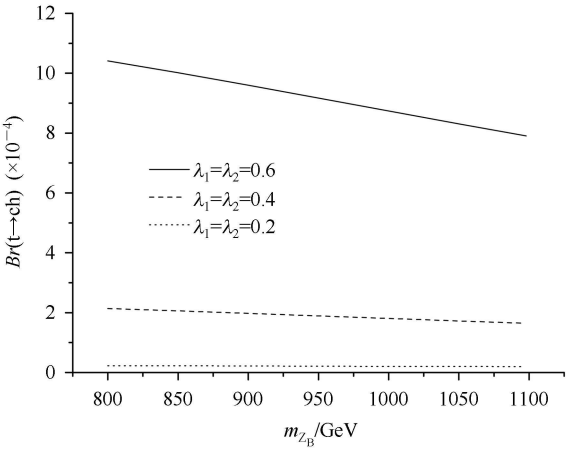

Fig. 4. The branching ratio of t→ch versus m_{Z_B}.

In Fig. 4, we plot the variation of $Br(t \to ch)$ with m_{Z_B}, adopting $m_{\tilde{Q}_4}$=790 GeV, μ_B=500 GeV, λ_Q=0.5, A_{BQ} = 1 TeV, and with $\lambda_1 = \lambda_2 = 0.6$ (solid line), $\lambda_1 = \lambda_2 = 0.4$ (dashed line), and $\lambda_1 = \lambda_2 = 0.2$ (dotted line). We can see that the BRs decrease as m_{Z_B} runs from 800 GeV to 1100 GeV, since m_{Z_B} contributes to the mass matrix of exotic squarks, and increase when $\lambda_1 = \lambda_2$ increases. When $\lambda_1 = \lambda_2$=0.6 or 0.4, $Br(t \to ch)$ is of the order of 10^{-4}; when $\lambda_1 = \lambda_2$=0.2, $Br(t \to ch)$ is of the order of 10^{-5}.

We assume $m_{\tilde{Q}_4}$=790 GeV, m_{Z_B}=1 TeV, λ_Q=0.5, and A_{BQ}=1 TeV. We plot in Fig. 5 the BRs of $t \to ch$ versus μ_B, with the solid line, dashed line and dotted lines corresponding to $\lambda_1 = \lambda_2$=0.6, 0.4 and 0.2 respectively. We can see that the BRs increase as μ_B runs from 300 GeV to 600 GeV, since μ_B is inversely proportional to the mass of the exotic squarks.

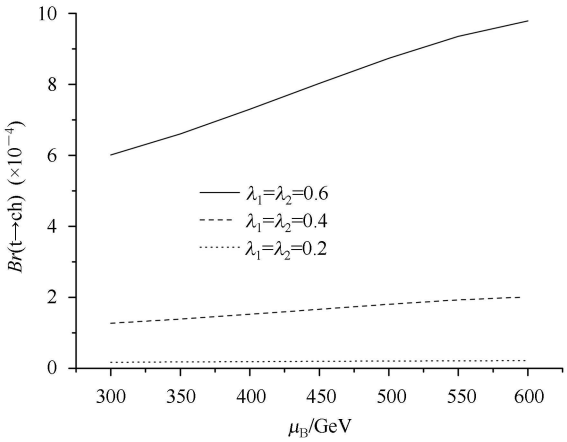

Fig. 5. The branching ratio of t→ch as a function of μ_B.

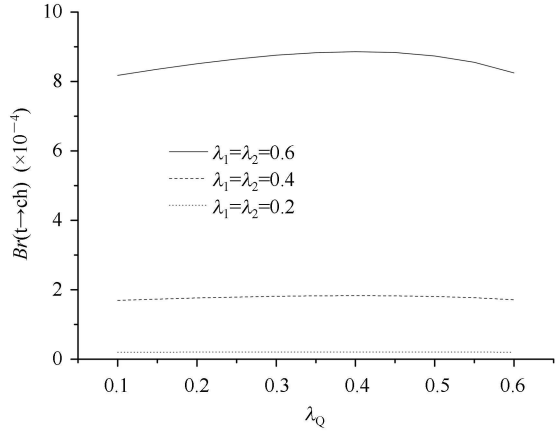

Fig. 6. Variation of t→ch branching ratio with λ_Q.

Choosing $m_{\tilde{Q}_4}$=790 GeV, m_{Z_B}=1 TeV, μ_B=500 GeV and A_{BQ}=1 TeV, we draw the variation of $Br(t \to ch)$ with λ_Q in Fig. 6 for $\lambda_1 = \lambda_2 = 0.6$,0.4 and 0.2 respectively. We can see that the curve first increases and then decreases, but not significantly, since λ_Q contributes both to the mass of exotic squarks and to the coupling coefficient.

Taking $m_{\tilde{Q}_4}$=790 GeV, m_{Z_B}=1 TeV, μ_B=500 GeV and λ_Q=0.5, we show the variation of $Br(t \to ch)$ with A_{BQ} in Fig. 7 for $\lambda_1 = \lambda_2$=0.6 (solid line), $\lambda_1 = \lambda_2$=0.4 (dashed line) and $\lambda_1 = \lambda_2$=0.2 (dotted line). We can see

that the BRs decrease as $A_{\rm BQ}$ runs from 1 TeV to 1.8 TeV, since $A_{\rm BQ}$ contributes to the mass matrix of exotic squarks. When $\lambda_1=\lambda_2=0.6$ or 0.4, $Br(\rm t\to ch)$ is of the order of 10^{-4}; when $\lambda_1=\lambda_2=0.2$, $Br(\rm t\to ch)$ is of the order of 10^{-5}.

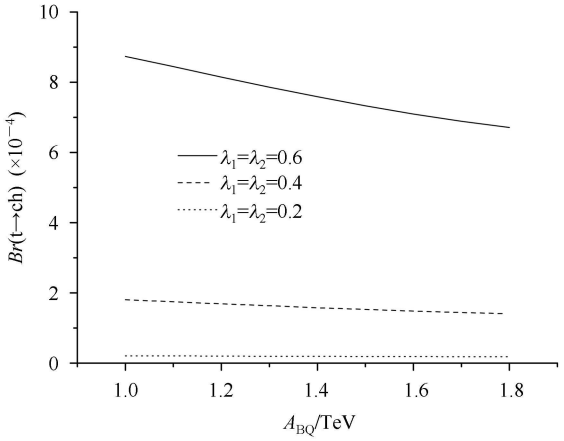

Fig. 7. The branching ratio of t→ch versus $A_{\rm BQ}$.

5 Summary

The LHC is a top-quark factory, and provides a great opportunity to seek out top-quark decays, with earlier work showing that the channel t→ch could be detectable, reaching a sensitivity level of $Br(\rm t\to ch)\sim5\times10^{-5}$ [26, 27]. In the SM, however, the branching ratio of the process is so small, $Br(\rm t\to ch)\sim10^{-13}$ [8], which is too small to be measurable in the near future.

In this work, we study the rare top decay to a 125 GeV Higgs in the framework of the BLMSSM. Adopting reasonable assumptions on the parameter space, we present the radiative correction to the process in the BLMSSM, and draw some of the relationships between the BRs and new physics parameters. We find that the branching ratio of t→ch can reach 10^{-3}, so this process could be detected in the near future at the LHC.

In addition, the author of [28] gives an estimated upper limit of $Br(\rm t\to ch)<2.7\%$ for a Higgs boson mass of 125 GeV, by combining the CMS results from a number of exclusive three- and four-lepton search channels. ATLAS find the limit of $Br(\rm t\to ch)<0.83\%$ at 95% C.L. by searching for $\rm t\to ch$, with $\rm h\to\gamma\gamma$, in $\bar{\rm t}\rm t$ events [29, 30]. Our numerical evaluations indicate the BRs are highly dependent upon the parameters $\lambda_{1,2}$, the values of which can have a sizeable effect on $Br(\rm t\to ch)$. Considering the experiment upper bounds from CMS and ATLAS, the parameters $\lambda_{1,2}$ should not be too large under our assumptions of the parameter space.

As we can see above, the t→ch process may be found in the near future, and further constraints on BLMSSM can be obtained from more precise determinations.

References

1 CMS collaboration. Phys. Lett. B, 2012, **716**: 30
2 ATLAS collaboration. Phys. Lett. B, 2012, **716**: 1
3 Perez P, Wise M. JHEP, 2011, **08**: 068
4 Perez P, Wise M. Phys. Rev. D, 2010, **82**: 011901
5 Mele B, Petrarca S, Soddu A. Phys. Lett. B, 1998, **435**: 401
6 Eilam G, Hewett J, Soni A. Phys. Rev. D, 1998, **59**: 039901
7 Eilam G, Hewett J, Soni A. Phys. Rev. D, 1991, **44**: 1473
8 Guasch J, Solà J. Nuclear Physics B, 1999, **562**: 3
9 CAO J C, HAN C C, WU Lei et al. Eur. Phys. J. C, 2014, **74**: 3058
10 Rosiek J. Phys. Rev. D, 1990, **41**: 3464
11 FENG T F, YANG X Y. Nucl. Phys. B, 2009, **814**: 101
12 Nilles H. Phys. Rept., 1984, **110**: 1
13 Haber H, Kane G. Phys. Rept., 1985, **117**: 75
14 Minkoski P. Phys. Lett. B, 1977, **67**: 421
15 Mohapatra R, Senjanovic G. Phys. Rev. Lett., 1980, **44**: 912
16 Perez P. Phys. Lett. B, 2012, **711**: 353
17 Arnold J, Perez P, Fornal B et al. Phys. Rev. D, 2012, **85**: 115024
18 http://cms.web.cern.ch/org/cms-papers-and-results
19 https://twiki.cern.ch/twiki/bin/view/AtlasPublic/SupersymmetryPublicResults
20 Perez P, Spinner S. Phys. Lett. B, 2014, **728C**: 489
21 Perez P, Wise M. Phys. Rev. D, 2011, **84**: 055015
22 Butterworth J, Ellis J, Raklev A et al. Phys. Rev. Lett., 2009, **103**: 241803
23 FENG T F, ZHAO S M, ZHANG H B et al. Nucl. Phys. B, 2013, **871**: 223
24 ZHAO S M, FENG T F, YAN B et al. JHEP, 2013, **1310**: 020
25 Denner A. Fortschr. Phys., 1993, **41**: 307
26 Aguilar-Saavedra J, Branco G. Phys. Lett. B, 2000, **495**: 347
27 Eilam G, Gemintern A, HAN T et al. Phys. Lett. B, 2001, **510**: 227
28 Craig N, Evans J, Gray R et al. Phys. Rev. D, 2012, **86**: 075002
29 ATLAS collaboration. ATLAS-CONF 2013, 081
30 CHEN K F, HOU W S, KAO C et al. Phys. Lett. B, 2013, **725**: 378